Ranjeet Kumar[1,*],

Omveer Singh[1],

Shailendra Kumar[2]

A Novel PV-UPQC Design for Voltage Control Utilizing AM-LMS Based Adaptive Controllers

JES Journal of Electrical Systems

Abstract: This study proposes an approximate multiplier least mean square (AM-LMS) controller based adaptive algorithm for compensating the power quality (PQ) issue and controlling the DC-link voltage of a unified power quality conditioner (UPQC) system. The suggested adaptive (AM-LMS) in order to execute in the operation. Consequently, compared to the traditional (AM-LMS), an optimal solution is achieved faster and with more accuracy. The suggested adaptive algorithm based on approximate multiplier the ideal DC-link regulating voltage. As a result, an ideal line voltage is introduced and the UPQC performance is enhanced against the PQ issue. Customers and suppliers are typically directly impacted financially by the quality of the power. Issues with electricity quality are caused by rising customer expectations. Power quality issues such voltage sag, swell, harmonics, and interruptions can have serious technical and financial effects on a large number of users. The primary topic of this work is UPQC, which combines shunt and series active power filters. Whereas shunt APF reduces distortions based on current, series APF reduces distortions based on voltage. UPQC mitigates distortions that are contingent upon voltage and current, both sequentially and independently. UPQC improves power quality by generating sinusoidal source current and load voltage at the appropriate voltage level, thereby compensating for both harmonics and load current. As a result, the PQ problem receives significant compensation. Crossover and mutation operations are performed in relation to the fitness function in the suggested adaptive algorithm. Additionally, the suggested UPQC system relies on an adaptable (AM-LMS) controller based controller is put into practice using the MATLAB environment, and the output's performance is assessed.

Keywords: AM-LMS, Harmonics, unified power quality conditioner, active power filter, and power quality.

1. Introduction

Solar energy generating is a fashionable way to produce ecologically friendly electricity in developing nations. This is particularly true in underdeveloped nations. Integrating energy from alternative sources likes wind and solar, in electrical distribution networks is growing as a result of government legislation and technological developments. Widespread deployment of renewable energy plants may interfere with electrical distribution networks' regular operations; therefore, their environmental effect has to be assessed. The grid typically inject active electricity to satisfy grid demands while functioning in island mode; hence, these power plants need to be able to employ both active and reactive power to fulfill their load requirements. A wide range of different tasks may be carried out by grid-connected power plants, while active energy generation is the main focus of daily research. By allowing for inaccurate calculations, approximate computing improves the performance of digital circuitry [1]. The mistakes resulting from approximations cause a manageable quality reduction in error-resilient applications. Multimedia processing is an example of an error-resistant application, where little errors may be accepted because of the limitations of human perception [2]. Furthermore, computational mistakes can be lessened by applications like recognition, mining, and synthesis that demand a respectable range of outcomes rather than a single "perfect" output [3-4]. The foundation for adaptive filtering, which is a standard in DSP applications for adaptive noise cancellation, the system identification, and channel adaptive equalization. Numerical stability, acceptable convergence error, and computing simplicity are all demonstrated by the LMS method [5]. Because of its intrinsic stability, a FIR filter often makes up an LMS adaptive filter technique, with the updating the filter's coefficients (Fig.1). The primarily responsible for the LMS algorithm's decreased complexity [6], which was the subject of several articles (Fig.1).

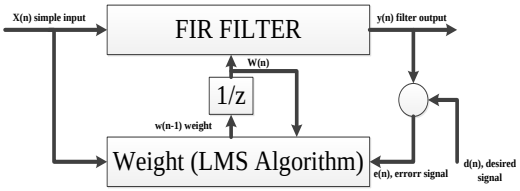

Fig 1 adaptive LMS filter

Which enables pipelined units to replace around 50% of multipliers? The use of Distributed Arithmetic to lower power dissipation and area occupation is investigated. In [10], the LMS algorithm's critical path is examined. Here, the authors note that while Delayed-LMS (DLMS) can be used when high sampling rates are needed (for as in radar applications), this algorithm is necessary for the most realistic scenarios. Using the SPT format, within the sign-LMS family [11-12], the goal of the recursive LMS method is to reduce the mean-

square-error (MSE) between a desired signal and the output of the FIR filter. The so-called gradient noise is caused by the LMS algorithm's approximate computation of the MSE gradient, which is necessary for reduction. As a result, the LMS algorithm has an intrinsic level of noise and is a good candidate for using approximation hardware circuits. This is the first time adaptive LMS filtering has been studied in connection with approximation circuits such as [13]; as far as the authors are understand. The most often performed operation in adaptive filters; we suggest using approximation multipliers in the adaptive filter's FIR portion. Proposed are truncated multipliers in [16]. To reduce the ensuing approximation error, a compensation term is used after the multiplier partial product matrix's least significant columns are eliminated. Using a presumptive 2x2 multiplier block, an approximation multiplier is examined in [17]. In order to reduce the maximum error, [18] modifies the approximation multiplier that was suggested in [18]. Three approximation multipliers are presented in [19], Similar to [20], in [21] using least significant column truncation and approximation compression using OR gates. Additionally, [22] uses mean error compensation. According to the research, the algorithm's stability and convergence performance may be jeopardized if the approximation multiplier topology is not properly chosen because of the feedback path. To maximize the error-performance trade-off, we suggest a variant of the multiplier in [23]. With tolerable convergence error degradation, the proposed circuits show multiplier reduces power consumption by 29%. In this study develops a method for a three-phase UPQC based on AM-LMS control. Even in cases when the voltage is severely distorted, the AM-LMS is positioned in front of the filter to produce sinusoidal waveforms that nearly resemble the input signal. This guarantees the PLL and the UPQC system quick and distortion-free functioning. The initial condition may be used to determine the fundamental components of the current voltage and angle hence the computational load is comparatively light. As a result, this approach is quick and easy. Two sets of AM-LMS are used to extract the fundamental positive sequence components (FPSCs) from the common coupling point bus; they also aid in the construction of reference signals for both APFs.

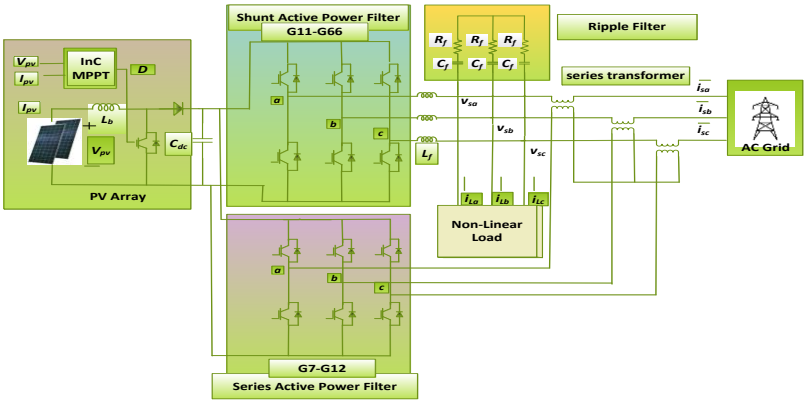

Fig 2. Proposed system configuration

2. A SHORT ANALYSIS OF THE LMS SYSTEM

Assume an M-taps FIR filter with tap inputs $\Phi(n) = [\Phi(n), \Phi(n-1), ...\Phi(n-m+1)]$ and tap weights $w_k(n)$, k $\in \{0\ldots M-1\}$. The results at each, the expression for time instant n is:

$$y(n) = \sum_{k=0}^{m-1} w_k(n), \Phi(n-k) \qquad (1)$$

Take note that the weights that are part in equation (1) are an expression of time instant n, in contrast to non-adaptive FIR filters. The error signal $e(n)$ in adaptive LMS filters is defined as the difference between the intended signal $d(n)$ and the actual filter response $y(n)$

$$e(n) = d(n) - y(n) \qquad (2)$$

The LMS method determines the updated version of the filter tap weights $w_k(n)$ based on the error $e(n)$ as follows:

$$W_k(n+1) = W_k(n) - \mu e(n)\Phi(n-k) \quad (3)$$

In which μ is the step-size parameter, establishing equilibrium between the algorithm's converging error and speed Note that the cost function is approximated [24] by the expression $\mu e(n)$.

$\Phi(n-k)$ .and $J(n) = E[|e(n)|]$ being E, the operation for statistical expectations. As a result, the LMS algorithm approximates the gradient (gradient noise) to minimize the MSE cost function; the adaptive filter explained by (1) is seen from a circulatory point of view because it demonstrates quicker convergence and fewer registers than its transpose-form equivalent, the direct form FIR filter is used in this study [10]. Additionally, μ, the step-size parameter, is selected as a power of two, in order to apply a hardwired shift to the matching multiplication operation.

3. APPROXIMATE MULTIPLIERS

In [18] and [20] to the signed situation as signed multipliers are frequently required in real-world DSP applications (such LMS filtering). Fig. 3 displays of the newly proposed approximation multipliers. The Kulkarni [18] estimated multiplier is displayed. Its foundation is an estimate multiplier block that computes an approximation sum from four partial products that pertain to three neighboring columns, yielding three output bits. Each blocks greatest and least important partial product is provided as output in its original form. To implement the approximation multiplier, the block is duplicated across the PPM. As mentioned in [18], precise blocks in the multiplier PPM's most important columns can be used to adjust the error-performance trade-off. Similar to the Kulkarni multiplier, it is made up of the repetition of approximation blocks, although each block is more intricate than the Kulkarni one. By using two XOR and one AND gate, although the maximum error is reduced, the electrical capacity is deteriorated and the error probability is increased.

Which is uses OR gates rather than half-adders to compress the partial products and lower the PPM height? It should be noted that OR gates with two-three and four inputs were utilized as compressors to create a single bit in the original version of the study. Since the approximation error in the other configurations is too high for the suggested application, we will only look at the situation of a 2-input OR gate in the following. The approximate multiplier of is displayed In this case, the compression strategy is comparable to [20], but the least important PPM columns are trimmed to enhance the electrical performance. A constant factor is used to compensate for the ensuing mean error, the error probability is [21] if the input bits of the two multiplier inputs are independent and have a 50% chance of being '1' When NAND partial products are used in the compression, the error probability increases thrice. Thus we see that, from the three phase load current component (W_{La},$W_{Lb,}$ W_{Lc}), the load value of the original active component can be calculated as,

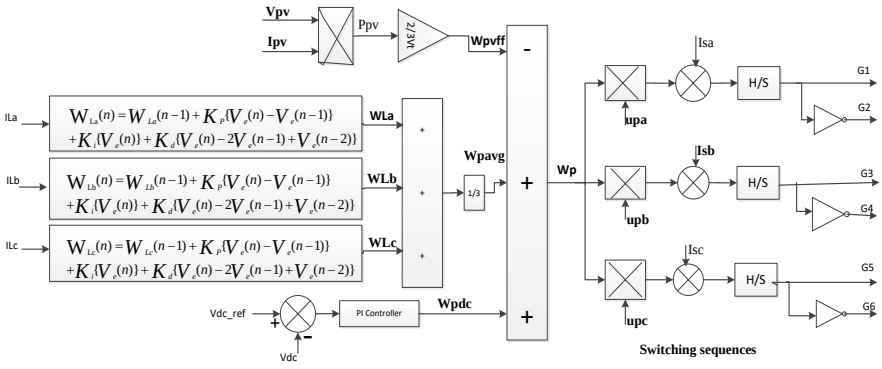

Fig 3. Approximate multipliers (AM-LMS) proposed algorithm

$$V_t = \sqrt{\frac{2(v_{sb}^2 + v_{sb}^2 + v_{sc}^2)}{3}} \quad (4)$$

As $v_{sca} = -v_{sab} + v_{sbc}$ thus by sensing the two line voltage phase voltage

$$v_{sa} = \frac{(2v_{sab} + v_{sbc})}{3}, \quad v_{sb} = \frac{(-v_{sab} + v_{sbc})}{3}, \quad v_{sc} = \frac{(-v_{sab} + 2v_{sbc})}{3} \tag{5}$$

The in phase and quadrature unit template are assessed follows

$$u_{pa} = \frac{(v_{sab} - v_{sca})}{3v_t}, \quad u_{pb} = \frac{(v_{sbc} - v_{sab})}{3v_t}, \quad u_{pc} = \frac{(v_{sca} - v_{sbc})}{3v_t}, \tag{6}$$

The extraction of weight values is comparable to the basic reactive components of three-phase load current weight (w_{pa}). The equation of average weight component for each phase of the active load is denoted by W_{pavg}. The average power load weight component is determined individually for each phase and is provided in the form W_{Pb}, W_{Pc}. Additionally PI (proportional-integral) controllers provide regulation on the AC side respectively. The estimated voltage at terminal V_t amplitude, is In order to generate a frequency error signal for frequency regulation and the frequency reference is linked to the frequency measured. The frequency inaccuracy is shown as (w_{pavg}) is then subtracted from frequency output controller (*wpdc)* then approximating the net fundamental weight is given equation.

$$W_{La}(n) = W_{La}(n-1) + K_P\{V_e(n) - V_e(n-1)\} + K_i\{V_e(n)\} + K_d\{V_e(n) - 2V_e(n-1) + V_e(n-2)\} \tag{7}$$

$$\text{Where} \quad V_e(n) = V_{dc}^* - V_{dc} \tag{8}$$

Where V_{dc}* is the three-phase reference voltage magnitude at the PCC and V_t is the AC supply voltage magnitude at the PCC. Additionally, the terminal weight voltage controller output (W_{PC}) is subtracted from the reactive fundamental load average output (W_{Pavg}), yielding the net fundamental weight is estimated as

$$wp = wpdc + wpavg - wpvff \tag{9}$$

Consequently, these errors in current signals (isae, isbe, and isce) are assigned to the hysteresis current controlle r for the formation of gating signals of IGBT's of VSC. Where the W_{Pavg} is the average reactive load weight component per phase is evaluated as,

$$W_{Pav} = \frac{W_{La} + W_{Lb} + W_{Lc}}{3} \tag{10}$$

The in-phase and quadrature reference currents are therefore seen as,

$$i_a^* = w_{pnet} \times u_{pa}, i_b^* = w_{pnt} \times u_{pb}, i_c^* = w_{pnet} \times u_{pc}, \tag{11}$$

The total reference currents (i_a*,i_b*,i_c*) are estimated as, Hence, for generation of gating signal of IGBT of VSC, these errors in the current signal (i_{sa}, i_{sb}, i_{sc}) are set to the hysteresis current controller. The measured current is, which is obtained through a DC-link PI controller. The PWM pulse for the converter is created by evaluating the PI controller output (duty cycle) using a saw tooth signal. The shunt active filter of PV-UPQC generates switching pulses by comparing the produced reference currents with the actual detected current and feeding the error to the hysteresis current controller.

- **Series controller**

The load voltage, which has been transformed into a frame, is compared with the reference voltage, the controller produces signals. Later on, it is converted into a frame, as seen in Fig 2. A PWM controller generates the gating pulses. Depicts the series converter control system.

4. SIMULATION RESULTS

The impact of adding approximation multipliers to the Adaptive LMS filter is investigated in the following, taking into account the algorithm's performance. As well as the electrical performances.

5. Results analysis with Discussions

a. Dynamic behavior of Adaptive AM-LMS-based control is employed in UPQC.

A system identification application is taken in order to evaluate the algorithm's performance when approximations are included. The system to recognize is an AM filter, as seen in Fig 4. By modifying of the AM filter coefficients $W_k(n)$ to resemble of the filter response, the LMS method in this instance minimizes the error e(n).

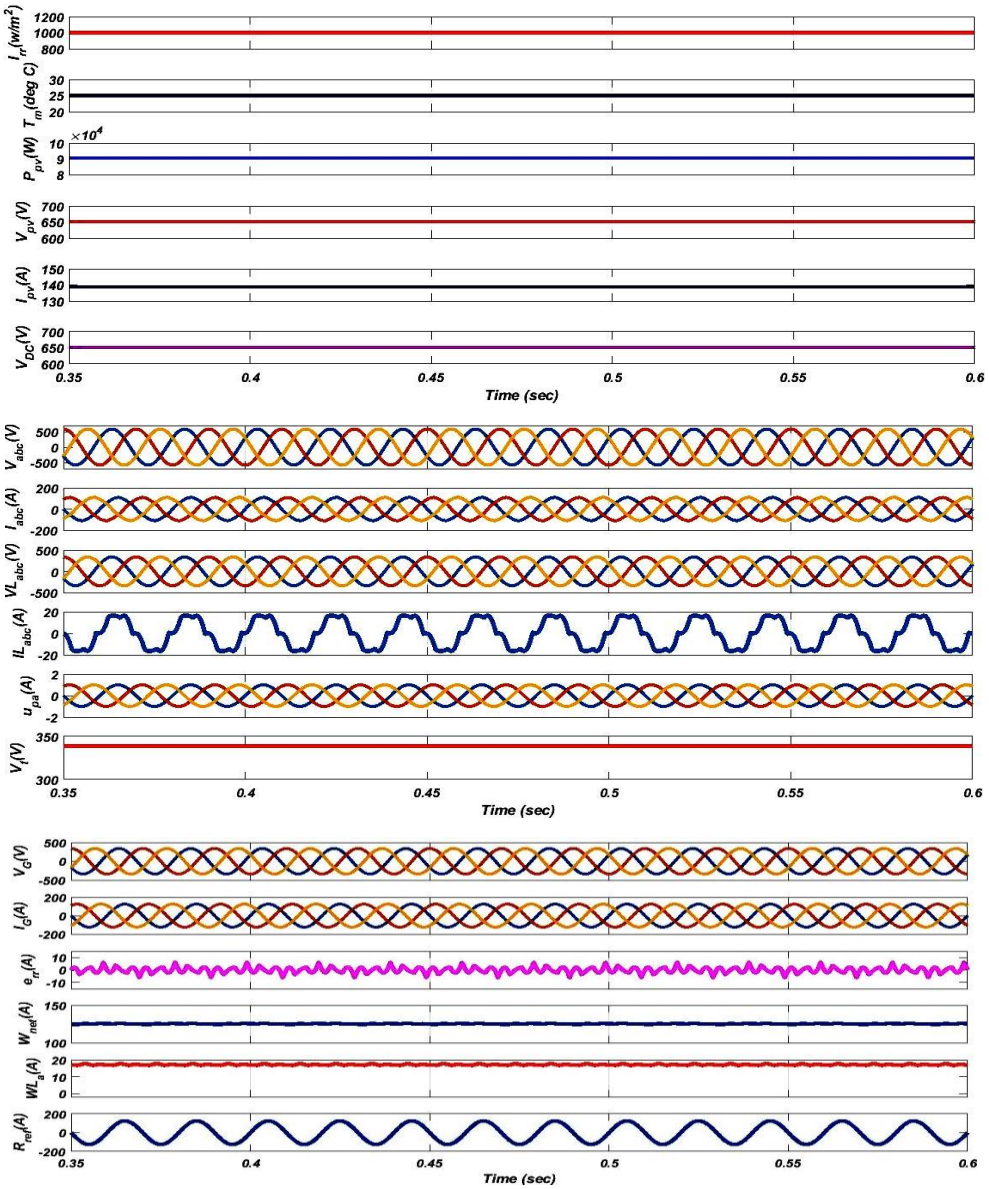

Fig. 4 The propose Steady state condition under nonlinear load condition v_{sab},i_{sa}, i_{sa},v_{sab} ,v_{vsc}, i_{vsc}, P_{vsc},v_{Lab} and i_{La} I_{pv},V_{pv}, P_{pv}

b. Results under Balanced and Unbalanced Non-linear loads

When the PV-UPQC system across various time periods as well as the increase in power quality in relation to these phenomena. Under load-unbalanced situations, both real power and reactive power can fluctuate; Fig.5 shows this shift in power flow between 0.5 and 0.25 seconds unbalance and 0.55 and 0.6 seconds balanced, respectively. There is a 0.2p.u. Drop in system voltage. Look when a single phase load is abruptly removed, load unbalancing occurs at P_{CC1}, as seen in Fig.5 When a single phase load is disconnected, the load power consumption is decreased. The corresponding phase 'a' current is kept sinusoidal even in the presence of abrupt load removal and addition. Sinusoidal under the current dynamic conditions is depicted in this picture.

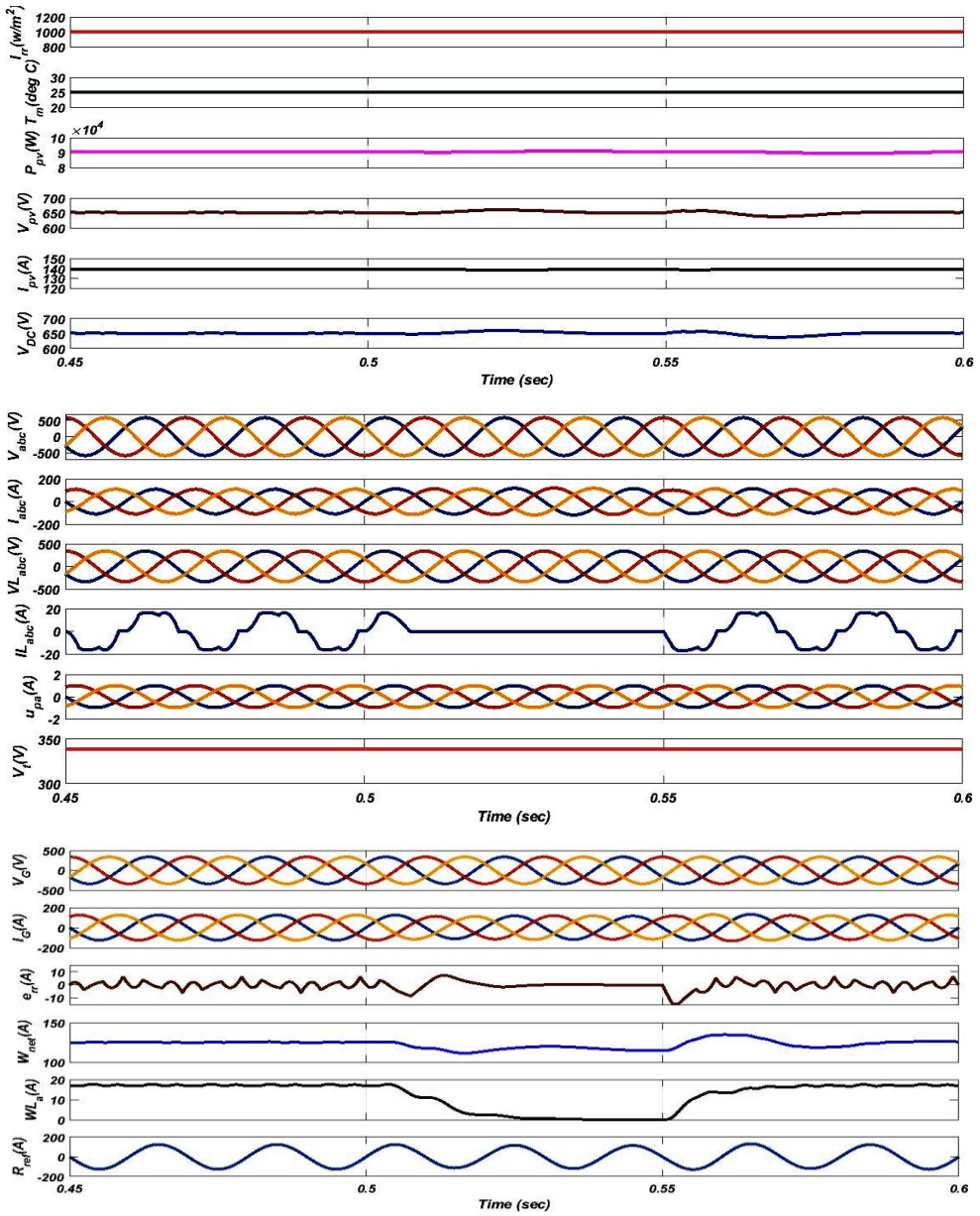

Fig 5. The proposed under Nonlinear Load Unbalance System

c. Performance When Sunlight Irradiation Vary

This section has looked at how the PV system behaves in dynamic situations with oscillations in solar radiation. The system solar irradiation conditions show the drop in solar irradiation from 1000 to 500 W/m2. Fig.6 makes it evident how the grid current at P_{CC1} decreases as the radiation decreases.

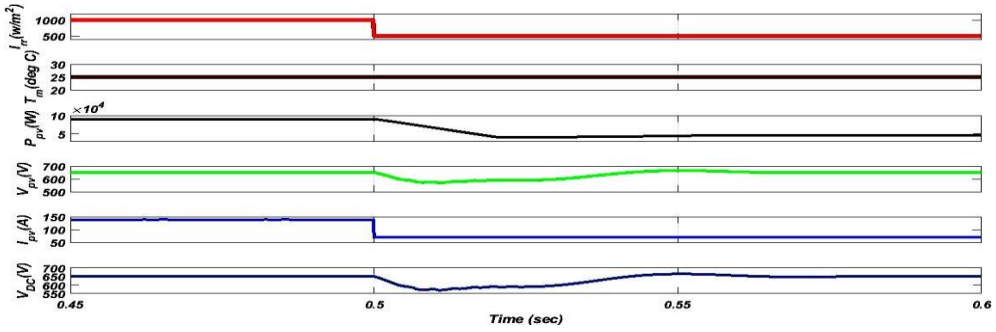

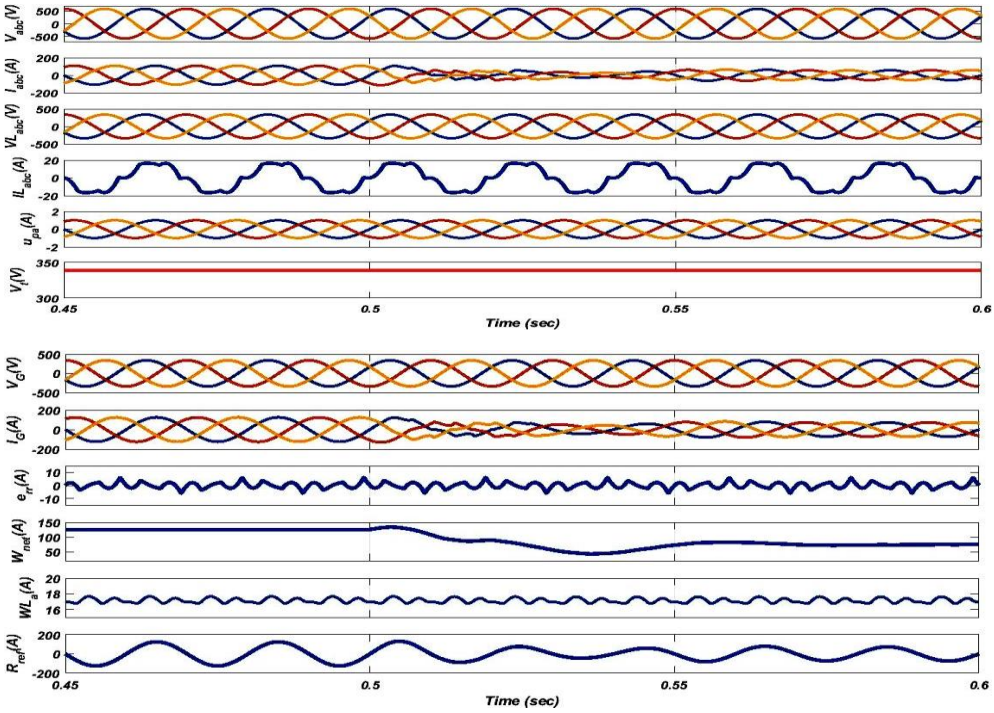

Fig.6 Under dynamic performance V_{dc}, i_{La}, v_{sab} & I_{pv} i_{sa}, P_{pv} , *Vvsc*, I_{vsc} under solar insolation change

6. TEST RESULT OF HARDWARE

In this the purpose of validating the control and model under study in simulation, a test setup is created in the OPL-RT. A PV-UPQC system prototype that makes use of coupled nonlinear loads and a voltage source converter has been developed. Power analyses and a digital storage oscilloscope were used to analyze the PV-UPQC's performance. The effectiveness and performance of the created system under various dynamic situations have been analyzed and validated through extensive tests using the parameters indicated.

A. Performance When Solar Irradiation Vary

This section illustrates how the system behaves when the PV array's solar intensity level drops from 1000 W/m2 to 500 W/m2. Along with the DC bus voltage being maintained stable at 650V, variations in the grid currents, VSC currents, and PV array currents are noted. Fig.7(a-b) also shows the changes in the intermediate signals as the weight of the Photovoltaic power component (P_{pv}), the Load current (I_L), and the overall weight of the active power component all climb in proportion to the increase in solar insolation.

(a) (b)

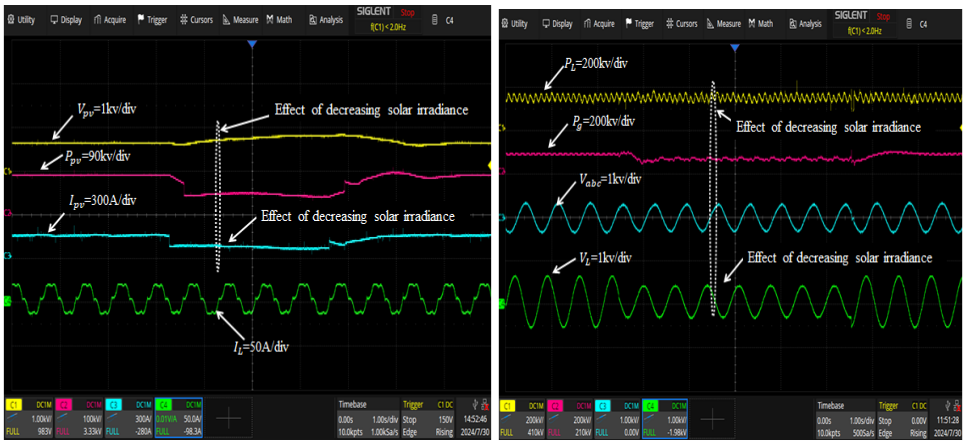

© (d)

Fig. 7 shows how the conditions of solar radiation vary: (a-b) irradiation and current decrease, (c-d) irradiation and current increase.

B. Appearance of Dynamic Performance under Load Unbalancing Conditions.

When a single phase load is abruptly removed, load unbalancing occurs at P_{CC1}, as seen in Fig.8 When a single phase load is disconnected, the load power consumption is decreased. In order to the structure's steady state behavior under balanced nonlinear loads by detaching the load from phase ‘a’ demonstrates the system's dynamic behavior when the load is out of balance. It is noted that the load is currently consuming less electricity, the grid currents are still balanced, and their magnitudes have grown. Additionally, Figs.8 shows the fluctuation of the intermediate signals.

(a) (b)

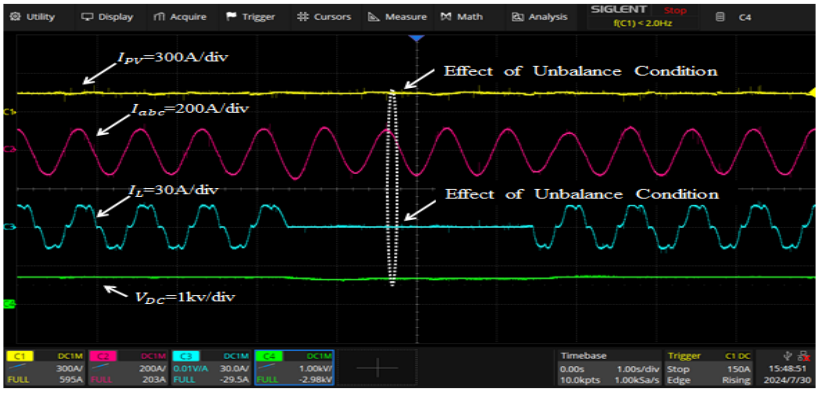

©

Figure 8: Unbalanced dynamic load condition: (a-b) abrupt load reduction, (c) abrupt load increase.

C. Dynamic Performance under Abnormal Voltage Conditions

According to analyses of Figs. 9 (b) and (c), respectively, the SRF controller and AM-LMS controller do not provide enough compensation for the load voltage's imbalance state. Fig.9 shows that the load voltages have reached a balanced state following the application of the suggested adaptive controller to the series compensator. It is determined from the findings that the suggested controller for the series compensator performs better than the others. An unbalanced voltage-sag is produced, where the phase 'a' voltage is lowered to 0.8p.u. in order to confirm the system's performance under fault conditions. Fig. 9 illustrates the dynamics of the PV array current, voltage, and inverter current after an abrupt drop in grid voltages. The operating point shifts to the right of the PV characteristic curve, resulting in an increase in PV array voltage and a decrease in PV array power. It is very desirable to control the load voltage in order to safeguard the voltage-sensitive loads under abnormal voltage situations at the PCC point. The system under consideration to a variety of voltage disturbances, including voltage sags, voltage swells, and voltage imbalances. As seen in Fig. 9 the voltage signals at PCC have been measured, and the voltage sag ranges from nominal 415 to 200V shows how well the system performs under sag conditions to control the load voltages. The load and dc-link voltages were effectively controlled by the system under consideration and to keep the balance of active power, there must

(a) (b)

Figure 9. (a-b) Condition of dynamic voltage sag: P_{CC1} voltage, load voltage regulation, series VSC injected voltage, dc-link voltage, P_{CC1} current, and PV array current.

Table.1 Comparison of Traditional LMS Control Algorithms with the Suggested AM-LMS Based Control

Parameter	Abc and dq Control Scheme	LMS	AM-LMS
Type of Filter Used	Time-domain PLL Based	Adaptive Technique based filter	Adaptive Technique based filter
Complexity	High	Small	Small
Optimization Degree	Na	2nd order	4th order
Static error	Na	High	small
Oscillation	Medium	less	Very Less
Controller speed	Very high	high	Very high
Computational Load	high	Less	Less
MSE	Na	4.5%	3.73%
Settling time	Poor	Poor	Acceptable Good
THD in grid current	Medium	High	Low
Dynamic Response	Slow	Fast	Very Fast
Sensor requirement	Voltage-3(V_{sabc}) Current-4 (i_{Labc}),	Voltage-3 (V_{sabc}) Current-4 (i_{Labc})	Voltage-3 (V_{sabc}) Current-4 (i_{Labc})

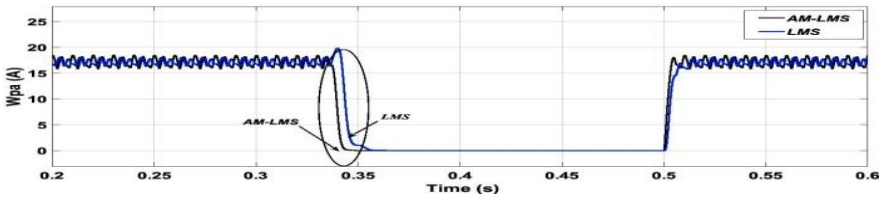

(a)

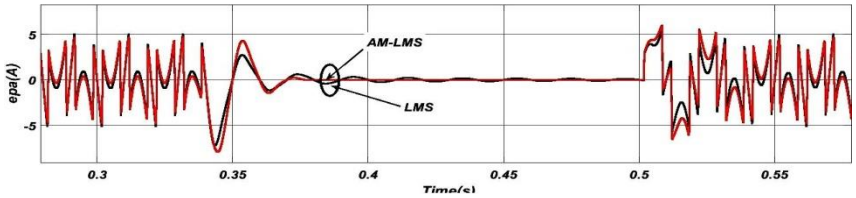

(b)

Fig 10(a-b) Comparison of Traditional LMS Control Algorithms with the Suggested AM-LMS Based Control

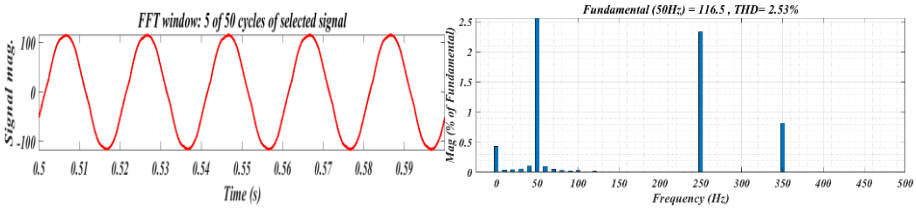

(a) (a')

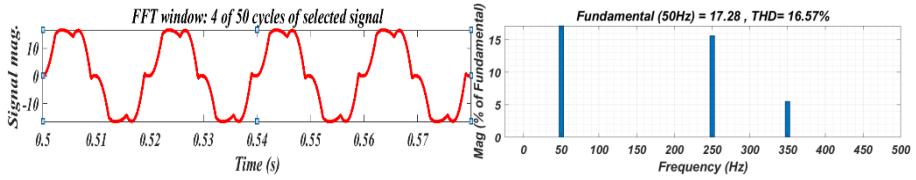

(b) (b')

Fig 11. Grid Current (a-a') THD, load current, (b-b') of $i_{La}$are the test findings under nonlinear loads.

7. CONCLUSION

The creation and application of the suggested PV-UPQC were completed in this article. The goal was to eliminate current quality problems and increase power quality in the face of varied voltage quality problems. The end user can choose the power quality level that best suits their needs using the platform that the current system offers. Even with significant voltage aberrations, the AM-LMS based SRF controller was used to provide an appropriate reference signal. The suggested logarithmic absolute technique was able to calculate the active weight component of the basic load current. The possibility of both high and low frequency ripples has been disregarded by using MAF rather than LPF for dc bus voltage management. The suggested algorithm's legitimacy has been confirmed by the experimental findings. Furthermore, the collected test results supported the suggested topology's effectiveness and performance.

APPENDICES

Grid voltage: 415V, 50Hz,	**Interfacing inductor, L_f = 2.5mH**
Solar power (P_{PV}): 90kW	Sampling time, Ts = 1μs
DC-link capacitor: 2.5mF	Grid voltage, V_{LL} = 415V (rms).
Shunt inductance interface: 3mH	Interfacing inductance with series 3.1mH
A switching frequency of VSC: 10 kHz	DC-link PI controller gains Kp= 1, Ki= 2
Ns = 21; Np = 17;	the VSC PI for Kp = 1200, Ki= 800;
DC bus voltage, V_{dc} = 650V	Bus capacitor, C_{dc} = 6mF

Load Parameter	
Ripple filter, R_f = 5Ω and C_f = 10μF	DC PI controller, K_{pd} =0.23 and K_{id} = 0.2
PI controller For AC, K_{pt} = 0.57 and K_{it} = 0.1	adaptation constant, μ = 0.0003, i = 0.0002, e=5
Nonlinear load = 3-Phase diode bridge with R = 65Ω	L = 300mH

References

[1] H. Fujita and H. Akagi, "The unified power quality conditioner: the integration of series- and shunt-active filters," in *IEEE Transactions on Power Electronics*, vol. 13, no. 2, pp. 315-322, March 1998, doi: 10.1109/63.662847.

[2] V. Khadkikar, A. Chandra, A. O. Barry, and T. D. Nguyen, "Power quality enhancement utilising single-phase unified power quality conditioner: Digital signal processor-based experimental validation," *IET Power Electron.*, vol. 4, no. 3, pp. 323–331, 2011.doi.org/10.1049/iet-pel.2010.0031

[3] D. A. Fernandes, F. F. Costa, J. R. S. Martins, A. S. Lock, E. R. C. da Silva and M. A. Vitorino, "Sensitive Load Voltage Compensation Performed by a Suitable Control Method," in *IEEE Transactions on Industry Applications*, vol. 53, no. 5, pp. 4877-4885, Sept.-Oct. 2017, doi: 10.1109/TIA.2017.2715173.

[4] R. K. Govindarajan, P. P. Raghav and G. S. Ilango, "A dynamic voltage restorer with an improved PLL for voltage sensitive loads," *2014 International Conference on Power Signals Control and Computations (EPSCICON)*, Thrissur, India, 2014, pp. 1-6, doi: 10.1109/EPSCICON.2014.6887499.

[5] A. H. Abed, J. Rahebi, H. Sajir and A. Farzamnia, "Protection of sensitive loads from voltages fluctuations in Iraqi grids by DVR," *2017 IEEE 2nd International Conference on Automatic Control and Intelligent Systems (I2CACIS)*, Kota Kinabalu, Malaysia, 2017, pp. 144-149, doi: 10.1109/I2CACIS.2017.8239048.

[6] A. K. Jindal and A. Joshi, "A unified power quality conditioner for voltage regulation of critical load bus," *IEEE Power Engineering Society General Meeting, 2004.*, Denver, CO, USA, 2004, pp. 471-476 Vol.1, doi: 10.1109/PES.2004.1372840.

[7] M. Basu, S. P. Das and G. K. Dubey, "Experimental investigation of performance of a single phase UPQC for voltage sensitive and non-linear loads," *4th IEEE International Conference on Power Electronics and Drive Systems. IEEE PEDS 2001 - Indonesia. Proceedings (Cat. No.01TH8594)*, Denpasar, Indonesia, 2001, pp. 218-222 vol.1, doi: 10.1109/PEDS.2001.975314.

[8] M. Brenna, R. Faranda and E. Tironi, "A New Proposal for Power Quality and Custom Power Improvement: OPEN UPQC," in *IEEE Transactions on Power Delivery*, vol. 24, no. 4, pp. 2107-2116, Oct. 2009, doi: 10.1109/TPWRD.2009.2028791.

[9] A. Teke, M. E. Meral, M. U. Cuma, M. Tümay, and K. Ç. Bayindir, "OPEN unified power quality conditioner with control based on enhanced phase locked loop," *IET Gener. Transm. Distrib.*, vol. 7, no. 3, pp. 254–264, 2013.doi.org/10.1049/iet-gtd.2012.0275

[10] M. C. Falvo, M. Manganelli, R. Faranda and H. Hafezi, "Smart n-grid energy management with an open UPQC," *2016 IEEE 16th International Conference on Environment and Electrical Engineering (EEEIC)*, Florence, Italy, 2016, pp. 1-6, doi: 10.1109/EEEIC.2016.7555548.

[11] H. Hafezi and R. Faranda, "Open UPQC series and shunt units cooperation within Smart LV Grid," *2017 6th International Conference on Clean Electrical Power (ICCEP)*, Santa Margherita Ligure, Italy, 2017, pp. 304-310, doi: 10.1109/ICCEP.2017.8004832.

[12] J. Kotturu and P. Agarwal, "Performance analysis of Open UPQC using three level diode clamped multilevel inverter," *2016 IEEE 6th International Conference on Power Systems (ICPS)*, New Delhi, India, 2016, pp. 1-6, doi: 10.1109/ICPES.2016.7584121.

[13] T. Wei and D. Jia, "A new topology of OPEN UPQC," *2014 9th IEEE Conference on Industrial Electronics and Applications*, Hangzhou, China, 2014, pp. 1313-1318, doi: 10.1109/ICIEA.2014.6931371.

[14] B. Singh, C. Jain and S. Goel, "ILST Control Algorithm of Single-Stage Dual Purpose Grid Connected Solar PV System," in *IEEE Transactions on Power Electronics*, vol. 29, no. 10, pp. 5347-5357, Oct. 2014, doi: 10.1109/TPEL.2013.2293656.

[15] S. Devassy and B. Singh, “Control of a Solar Photovoltaic Integrated Universal Active Power Filter Based on a Discrete Adaptive Filter,” in *IEEE Transactions on Industrial Informatics*, vol. 14, no. 7, pp. 3003-3012, July 2018, doi: 10.1109/TII.2017.2778346.

[16] S. K. Dash and P. K. Ray, “Design and modeling of single-phase PV-UPQC scheme for power quality improvement utilizing a novel notch filter-based control algorithm An experimental approach,” *Arabian J. Sci. Eng.*, vol. 43, no. 6, pp. 3083–3102, 2018. doi.org/10.1007/s13369-018-3116-3

[17] S. Devassy and B. Singh, “Performance analysis of proportional resonant and ADALINE-based solar photovoltaic-integrated unified active power filter,” *IET Renewable Power Gener*., vol. 11, no. 11, pp. 1382–1391, 2017.doi.org/10.1049/iet-rpg.2017.0045

[18] S. Devassy and B. Singh, "Design and performance analysis of three-phase solar PV integrated UPQC," *2016 IEEE 6th International Conference on Power Systems (ICPS)*, New Delhi, India, 2016, pp. 1-6, doi: 10.1109/ICPES.2016.7584022.

[19] Yazdani, A. Bakhshai, G. Joos and M. Mojiri, "A Nonlinear Adaptive Synchronization Techniquefor Grid-Connected Distributed Energy Sources," in *IEEE Transactions on Power Electronics*, vol. 23, no. 4, pp. 2181-2186, July 2008, doi: 10.1109/TPEL.2008.926045.

[20] S. Devassy and B. Singh, “Discrete adaptive notch filter based single phase solar PV integrated UPQC,” *2016 IEEE 1st International Conference on Power Electronics, Intelligent Control and Energy Systems (ICPEICES)*, Delhi, India, 2016, pp. 1-5, doi: 10.1109/ICPEICES.2016.7853162.

[21] P. F. Ksiazek and M. Ordonez, “DC-Link Control Filtering Options for Torque Ripple Reduction in Low-Power Wind Turbines,” in *IEEE Transactions on Power Electronics*, vol. 32, no. 6, pp. 4812-4826, June 2017, doi: 10.1109/TPEL.2016.2597844.

[22] M. Ordonez, “Swinging bus technique for ripple current elimination in Fuel Cell power conversion,” *2011 IEEE Energy Conversion Congress and Exposition*, Phoenix, AZ, USA, 2011, pp. 3330-3335, doi: 10.1109/ECCE.2011.6064218.

[23] M. O. Sayin, N. D. Vanli and S. S. Kozat, “A Novel Family of Adaptive Filtering Algorithms Based on the Logarithmic Cost,” in *IEEE Transactions on Signal Processing*, vol. 62, no. 17, pp. 4411-4424, Sept.1, 2014, doi: 10.1109/TSP.2014.2333559.

[24] P. Shah, I. Hussain, and B. Singh, “Real-time implementation of optimal operation of single-stage grid interfaced PV system under weak grid conditions,” IET Gener. Transmiss. Distrib. Res., vol. 12, no. 7, pp. 1631–1643, 2018. doi.org/10.1049/iet-gtd.2017.0623

[25] M. O. Sayin, N. D. Vanli and S. S. Kozat, “A Novel Family of Adaptive Filtering Algorithms Based on the Logarithmic Cost,” in *IEEE Transactions on Signal Processing*, vol. 62, no. 17, pp. 4411-4424, Sept.1, 2014, doi: 10.1109/TSP.2014.2333559.

[26] S. Malarvili, S. Mageshwari, “Nonlinear PID (N-PID) controller for SSSP grid connected inverter control of photovoltaic systems,” *Electr. Power Syst. Res*. 211 (2022) 108175.doi.org/10.1016/j.epsr.2022.108175